JOURNAL OF BACTERIOLOGY, July 1988, p. 3094–3101
0021-9193/88/073094-08$02.00/0

Vol. 170, No. 7

Minicell-Forming Mutants of *Escherichia coli*: Production of Minicells and Anucleate Rods

ALINE JAFFÉ,[1]* RICHARD D'ARI,[1] AND SOTA HIRAGA[2]

Institut Jacques Monod, Centre National de la Recherche Scientifique and Université Paris 7, 2, Place Jussieu, 75251 Paris Cedex 05, France,[1] and Department of Molecular Genetics, Kumamoto University Medical School, Kumamoto 862, Japan[2]

The *Escherichia coli minB* mutant originally isolated is known to septate at cell poles to form spherical anucleate minicells. Three new minicell-producing mutants were isolated during a screening by autoradiography for chromosome partition mutants giving rise spontaneously to normal-sized anucleate cells. These *min* mutants were affected close to or in the *minB* locus. Autoradiography analysis as well as fluorescent staining of DNA showed that in addition to minicells, these strains and the original *minB* mutant also spontaneously produced anucleate rods of normal size and had an abnormal DNA distribution in filaments. These aberrations were not associated with spontaneous induction of the SOS response. Inhibition of DNA synthesis in these mutants gave rise to anucleate cells whose size was longer than unit cell length, suggesting that the *min* defect allows septation to take place at normally forbidden sites not only at cell poles but also far from poles. Abnormal DNA distribution and production of anucleate rods suggest that the Min product(s) could be involved in DNA distribution.

As an approach to understanding the regulation of cell division in *Escherichia coli*, we have been studying the mechanisms coupling division to DNA replication. When DNA synthesis is blocked, the SOS response is generally induced, including the division inhibitors SfiA (12, 13, 15) and (when present) SfiC (6), and cell division is rapidly arrested. In mutant strains in which these division inhibitors cannot operate, division is less strictly coupled to chromosome replication: when DNA synthesis is perturbed, although division is greatly reduced, 10 to 50% of the population segregates as anucleate rod-shaped cells, whatever the nature of the replication perturbation (18, 19). The production of these anucleate cells has been shown to require and to be modulated by cyclic AMP (cAMP) and the cAMP receptor protein (CAP) (19). The residual divisions responsible for anucleate cell production seem to take place at normal septation sites since the anucleate cells formed are rods of approximately normal size (19). This differentiates them sharply from anucleate "minicells," tiny spherical cells produced spontaneously either by the *minB* mutant (1) or by strains bearing a multicopy plasmid coding for the cell division protein FtsZ (36).

In the course of a search for mutants which spontaneously produce normal-sized anucleate cells, three clones were found to produce minicells, like the classical *minB* mutant. There was only one *minB* mutant known, isolated by Adler et al. (1). It produces anucleate minicells and nucleate cells, although never simultaneously (2), and the nucleate cells have a broad length distribution, including filaments (32). A single mutation is responsible for the minicell phenotype (8), although recent work has established that the locus is complex and that several genes are involved (9). Our three new minicell-producing mutants are affected at or near the *minB* locus; they also have a broad length distribution, although one allele produces fewer minicells and filaments. Analysis of the cell size distribution in a *minB* culture led Teather et al. (32) to propose a model in which the *minB*$^+$ product inactivates septation sites after septation has taken place. These authors suggest that in the *minB* mutant, cell poles (used septation sites) can be reused, resulting in formation of minicells; they further postulate that the number of divisions is limited to one per unit mass increase by the amount of a hypothetical division factor.

We report here several observations that are difficult to reconcile with the above model. The classical *minB* mutant and our three new *min* mutants produced anucleate rods as well as spherical minicells. These two populations of anucleate cells, spherical and rod-shaped, had broad size distributions which in fact overlapped. Autoradiography and fluorescent DNA staining revealed that spontaneous *min* filaments occasionally had DNA-free poles and an abnormal DNA distribution which could allow septa to be formed between the DNA mass and a cell pole. When DNA replication was blocked (in the absence of SOS-associated division inhibition), the anucleate cells formed included longer filamentous rods; this suggests that the *min* mutations may also allow the utilization of nonpolar sites not normally available for septation.

The division process that generates minicells seems to be normal, as judged by the fine structure of the septum observed with the electron microscope (1); furthermore, it is inhibited by nalidixic acid (5), which is known to induce the SOS-associated division inhibitor SfiA (13). To determine whether these aberrant divisions obey the same regulation as those producing anucleate rods, we studied minicell and anucleate rod production, both spontaneous and during a DNA replication block, in the presence and absence of a functional cAMP-CAP complex, with strains carrying the *minB* mutation or the three new *min* mutations. A functional cAMP-CAP complex was required for production of the anucleate rods but not of minicells, showing that these two types of aberrant division have different patterns of regulation.

MATERIALS AND METHODS

Bacterial strains. All strains used in this study were *E. coli* K-12 derivatives; they are listed in Table 1. GC2700, received from A. Ullmann, is a K-12 F$^-$ (λ)$^-$ prototroph that has not been subjected to multiple rounds of mutagenesis in

* Corresponding author.

TABLE 1. Bacterial strains

Strain	Genotype
GC2700	K-12 F^- $(\lambda)^-$, prototroph
GC2589	As GC2700, *thy deo*
GC7078	As GC2589, *ftsZ114* (SfiB)
GC7080	As GC2589, *ftsZ114* (SfiB) Δ*cya*
GC7082	As GC2589, *ftsZ114* (SfiB) Δ*cya minB1 zcf-117*::Tn*10*
GC7088	As GC2589, *ftsZ114* (SfiB) *minB1 zcf-117*::Tn*10*
GC7106	As GC2589, *sfiA85*
GC7111	As GC2589, *minB1 zcf-117*::Tn*10*
GC7115	As GC2589, *sfiA85 minB1 zcf-289*::Tn*5*
B1654	*thr his arg rpsL sfiA100*::Tn*5 sfiC srlC300*::Tn*10 thy deo*
B1688	As B1654, srl^+ *minB1 zcf-117*::Tn*10*
MT1	*ilv his rpsL* (λ *N7 N53* cI^+ cro^+::gal^+)
GC7142	As MT1, *minB1 zcf-117*::Tn*10*
LE316	*gyrB*(Ts) *arg ilv met thr his lac rpsL*
SH392	K-12, *met hsdR gal supE sfiC*
GC7237	As SH392, *sfiA85*
GC7240	As GC7237, *minB1 zcf-117*::Tn*10*
GC7245	As GC7237, *min-2 zcf-117*::Tn*10*
GC7246	As GC7237, *min-3 zcf-117*::Tn*10 zcf-289*::Tn*5*
GC7247	As GC7237, *min-4 zcf-117*::Tn*10*
GC7260	As GC7237, *thy zcf-117*::Tn*10*
GC7256	As GC7237, *minB1 thy zcf-117*::Tn*10*
GC7257	As GC7237, *min-2 thy zcf-117*::Tn*10*
GC7258	As GC7237, *min-3 thy zcf-117*::Tn*10*
GC7259	As GC7237, *min-4 thy zcf-117*::Tn*10*
GC7254	As GC7237, *minB1* Δ*cya ilv*::Tn*5 zcf-117*::Tn*10*
GC7255	As GC7237, *min-2* Δ*cya ilv*::Tn*5 zcf-117*::Tn*10*
GC7261	As GC7237, *min-4* Δ*cya ilv*::Tn*5 zcf-117*::Tn*10*

the laboratory. Strain B1654 has been described (19), as have MT1 (33), LE316 (11, 30), and SH392 (20, 29).

The *thy* auxotrophs were selected on trimethoprim (27), and the *deo* derivatives were spontaneous low-thymine requirers (3 μg/ml); strains GC7078 and GC7106 did not carry the same *deo* allele as GC2589. The *sfiA* (6, 12), *ftsZ* (SfiB) (12), *cya* (4), and *minB* (8) mutations were introduced by P1 transduction. The *minB*-linked transposon insertions *zcf-117*::Tn*10* and *zcf-289*::Tn*5* were kindly given us by L. Rothfield and G. Walker. The *min* transductants were detected by the presence of minicells and filamentous cells in cultures. The genotypes of these transductants at the closely linked *sfiC* locus (25) are not known, since the presence of spontaneous filaments made the usual test (6) difficult to read.

Media. Cells were grown at 37°C in LB broth (27) or in appropriately supplemented ME (34) or M63 (27) salts. Autoradiography experiments were carried out in minimal 63 medium (27) supplemented with glucose (0.4%), thymine (5 μg/ml), Casamino Acids (0.4%), and thiamine (10 μg/ml); [^{3}H]thymine (Amersham) was used at a specific activity of 4.4 Ci/mmol.

Antibiotics were used at the following concentrations: chloramphenicol, 50 μg/ml; trimethoprim, 10 μg/ml; tetracycline, 10 μg/ml; kanamycin, 20 μg/ml; and furazlocillin, 1.5 μg/ml. β-Lactamase, extracted from a pBR322-bearing strain, was kindly given us by L. Guttman; the extract was used at a 60-fold dilution.

Isolation of *min* mutants. Strain GC7106 was mutagenized in rich medium containing nitrosoguanidine (2 μg/ml) and aerated for 4 h at 37°C (27). The culture was plated on rich medium and incubated overnight at 37°C. Five hundred clones were transferred to M63 glucose medium containing [^{3}H]thymine and grown for 36 h at 37°C. Each clone was transferred with a toothpick to a 5-μl drop of 2% formaldehyde deposited on a microscope slide (the slide could hold 16 clones). Samples were then treated for autoradiography and analyzed for the presence of normal-sized anucleate cells.

Fluorescent DNA staining. The DNA staining technique developed by S. Hiraga will be published elsewhere (manuscript in preparation); briefly, it consists of observing 4,6-diamidino-2-phenylindole (DAPI)-stained bacteria through a fluorescence microscope under phase contrast by UV and visible light simultaneously. DAPI was purchased from Sigma Chemical Co.

Miscellaneous. Thymine starvation was carried out at 37°C. P1-mediated transduction (27), DNA extraction, transformation and preparation of competent cells (26), lysogenization with λ *sfiA*::*lac* (14), and β-galactosidase assays (27) have been described. The autoradiography method was described previously (18); it involved prelabeling with [^{3}H]thymine for a minimum of 15 generations.

RESULTS

Isolation and mapping of *min* mutants. Our initial purpose was to look for chromosome partition mutants which spontaneously produced normal-sized anucleate cells during growth. These were detected by autoradiography (see Materials and Methods), screening for the presence of anucleate rods in colonies. Among 10 clones showing the presence of anucleate rods, 5 were found to degrade their DNA, 3 produced minicells, and 2 had the phenotype expected of chromosome partition mutants and are under study. The technique used involved Giemsa staining, which does not color minicells sufficiently to permit unambiguous counting, although cells of normal size or larger, whether nucleate or anucleate, were clearly visible. Minicells, whose volume is about 1/10 that of normal cells (1), were observed by phase-contrast microscopy; although precise quantification proved difficult, the relative production of minicells was readily evaluated by counting polar septa, i.e., cell extremities with a minicell still attached by a deep constriction.

The three minicell-producing clones were found to carry mutations that were about 50% cotransducible with the transposon insertions *zcf-117*::Tn*10* and *zcf-289*::Tn*5*, which are closely linked to the *minB1* mutation at 26 min on the *E. coli* genetic map (8, 31). We call these alleles *min-2*, *min-3*, and *min-4* and that of Adler et al. (1) *minB1*. The new *min* alleles and the *minB1* mutation were transduced into different strains, and the transductants were analyzed by autoradiography and specific fluorescent staining of the DNA.

Spontaneous production of anucleate rods and minicells by *min* mutants. We measured the spontaneous frequency of anucleate rods in cultures of the three new *min* mutants during exponential growth by autoradiography and by specific fluorescent DNA staining. The *minB1* mutant, which has not previously been reported to produce anucleate rods, was analyzed in parallel. As shown in Table 2, less than 0.1% anucleate rods could be detected in the parental min^+ strain. In contrast, the four *min* mutants exhibited 1 to 10% anucleate rods. The presence of a $sfiA^+$ allele did not abolish anucleate rod production (Table 2, strain GC7111).

The spherical minicells produced by the three new mutants were anucleate, as judged by lack of fluorescence with

TABLE 2. Anucleate rod production

Strain and method	Relevant genotype	Anucleate rods[a] (%)	
		Spontaneous	Thymine starvation (4 h)
Autoradiography[b]			
GC7106	*sfiA*	≤0.2	NT
GC7111	*sfiA*$^+$ *minB1*	3.7	NT
GC7115	*sfiA minB1*	9.9	NT
GC7078	*ftsZ* (SfiB)	≤0.1	15
GC7088	*ftsZ* (SfiB) *minB1*	8.7	20
GC7080	*ftsZ* (SfiB) Δ*cya*	≤0.1	1.1
GC7082	*ftsZ* (SfiB) Δ*cya minB1*	0.8	1.7
Fluorescent staining[c]			
GC7260	*sfiA*	≤0.1	37
GC7256	*sfiA minB1*	4.6	30
GC7257	*sfiA min-2*	2.0	56
GC7258	*sfiA min-3*	1.4	32
GC7259	*sfiA min-4*	1.4	12

[a] The percentage of anucleate rods was scored by direct observation and on photomicrographs; 200 to 1,000 cells were scored per sample. NT, Not tested.
[b] Cultures were grown in M63 glucose–Casamino Acids–[^{3}H]thymine medium. Samples were prepared for autoradiography during exponential growth (spontaneous) and after 4 h of thymine starvation.
[c] Cultures were grown in ME glucose–Casamino Acids–thymine medium. Samples were stained with DAPI during exponential growth (spontaneous) and after 4 h of thymine starvation.

DAPI. In LB broth the proportion of polar septa and of minicells was found to be lower in the *min-2* mutant (2% polar septa) than in the three other mutants (10 to 18% polar septa), although cultures of all four mutants always contained more minicells than anucleate rods. Strain GC7245 (*min-2*) had a slower growth rate than the other *min* mutants. In this and other aspects (see below), the *min-2* allele was clearly different from the other three.

Cell size distribution in the *min* mutants. Measurements of the size distribution of nucleate cells on photomicrographs after DAPI staining revealed that the *min-3* and *min-4* mutants, like the classic *minB1* mutant, generated a wide range of lengths from normal size to filaments equivalent to six unit cell lengths. In contrast, the *min-2* mutant contained few filaments (Fig. 1).

The size distribution of anucleate cells measured after DAPI staining, including spherical and rod-shaped anucleate cells, was broader than expected, although no anucleate filaments were detected (Fig. 2). The distribution of minicell diameters actually overlapped that of anucleate rod lengths (Fig. 2). The mean length of the anucleate rods was slightly smaller than the mean length of nucleate *min*$^+$ cells (Fig. 1A and 2).

Distribution of nucleoids in filamentous cells. Autoradiography of *minB1* cells revealed some spontaneous filaments in which the DNA occupied the central region, with at least one (*min*$^+$) cell length between the DNA mass and the poles. These cells are presumably the progenitors of the anucleate rods observed.

The localization of the chromosomal DNA within cells was especially easy to see by DAPI staining of cells in which division had been inhibited by 60 min of treatment with furazlocillin (a β-lactam antibiotic) followed by a 60-min treatment with chloramphenicol, which allowed DNA replication cyles to terminate. In the four *min* mutants, 10 to 20% of such filaments clearly showed the same type of aberration observed spontaneously: either a large DNA mass in the center or several irregularly distributed DNA masses, with DNA-free poles (Fig. 3; unpublished observations). The parental *min*$^+$ strains, on the other hand, had a regular nucleoid distribution along the filaments, with only 1% showing an abnormal DNA distribution. Although the *min-2* mutant produced few filaments and few minicells spontaneously, it showed the same proportion of cells with an abnormal DNA distribution. The phenotype of *min* mutants is reminiscent of that of some *gyrB*(Ts) (30) and *gyrA*(Am) (16, 17) mutants, in which gyrase is inactivated at high temperature. At 42°C, these mutants, like the *min* mutants, generate minicells and anucleate rods with a broad length distribution and show an irregular nucleoid distribution in filaments (16, 30). Our experimental protocol (furazlocillin, chloramphenicol, DAPI), applied to the *gyrB*(Ts) mutant LE316 (30) after 2 h at 42°C, confirmed an abnormal DNA distribution in all filaments and a broad size distribution of minicells and anucleate rods, as described by Orr et al. (30).

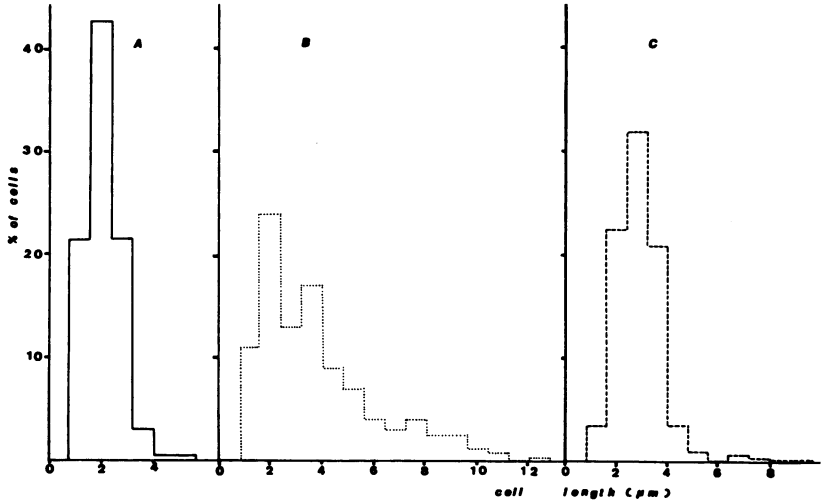

FIG. 1. Length distribution of nucleate cells during exponential growth in LB broth. Cell lengths were measured on photomicrographs of DAPI-stained bacteria. The strains used were (A) GC7237 (*min*$^+$), (B) GC7240 (*minB1*), and (C) GC7245 (*min-2*).

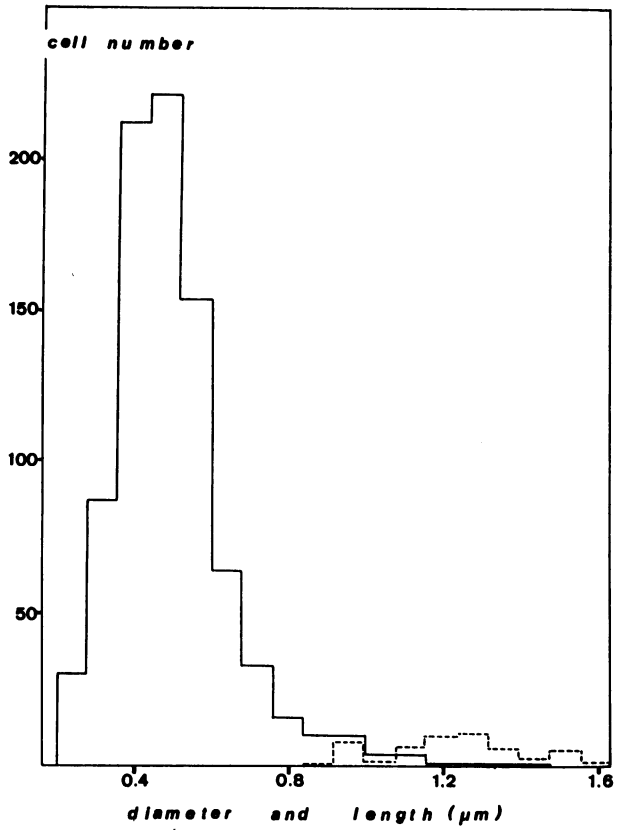

FIG. 2. Size distribution of minicells (——) and anucleate rods (-----) in *min* mutants. Minicell diameters and anucleate rod lengths were measured on photomicrographs of DAPI-stained cells. No significant differences were observed among the *min* mutants; the data from the four strains GC7256, GC7257, GC7258, and GC7259 were pooled.

The phenotypic similarity between *min* and *gyr* mutants suggests that DNA structure in the former may be altered.

Effect of transient cell division inhibition. Cultures of *min* mutants contain dividing filaments. To test whether this in itself is sufficient to cause aberrant division, we looked to see whether the production of anucleate rods could be induced in a wild-type strain by transiently inhibiting cell division and then releasing the block. We used the β-lactam antibiotic furazlocillin, which specifically and reversibly inhibits the essential division protein PBP3 (3). Strains GC7078 (*minB*$^+$) and GC7088 (*minB1*) were treated for 75 min with furazlocillin (1.5 μg/ml). Division ceased abruptly, whereas cell mass, measured by optical density, increased 3.2-fold. The division block was released by addition of β-lactamase to the cultures; division resumed within 15 min. [^{3}H]thymine-labeled samples were analyzed by autoradiography every 15 min for 90 min. The *minB1* culture contained 6 to 8% anucleate rods throughout the resumption of division, showing that such cells were formed at about the same rate as nucleate cells. In the *minB*$^+$ strain, no anucleate rods were found during the period of resumption (<0.2%), showing that filaments in which the DNA is regularly distributed do not normally divide to produce anucleate cells. This result further shows that furazlocillin treatment does not cause abnormal DNA distribution. Thus, the presence of dividing filaments is not sufficient to produce anucleate cells. Anucleate cell production is correlated with, and may require, the presence of dividing filaments whose nucleoid distribution is faulty.

Inhibition of DNA synthesis. In *minB*$^+$ strains, anucleate rods are not generally produced spontaneously but appear together with filaments when DNA synthesis is perturbed in the absence of SOS-associated division inhibition (18, 19, 28). To follow their production under these conditions in *min* mutants, we introduced the *min* mutations into *sfiA* and *ftsZ* (SfiB) strains, in which the FtsZ protein (the normal target of SOS-associated inhibition [22]) is no longer sensitive to the SfiA and SfiC division inhibitors (6, 21, 24). We then blocked DNA chain elongation by thymine starvation. In all cases, cell division was partially inhibited under nonpermissive conditions, and anucleate rods accumulated to similar levels in *min* and *minB*$^+$ strains, reaching 15 to 50% of the population, excluding minicells (Table 2).

Minicell production during thymine starvation was observed in the *minB* strain B1688 by phase-contrast microscopy on a parallel unlabeled culture. Samples were fixed in 2% formaldehyde, and the percentage of cells with polar septa was measured; it decreased from 11% at time zero to 2.9 and 1.5% after 2 and 4 h of thymine starvation, respectively. Bacteria with nonpolar septa were also scored; there were 8.7% initially, with 2.4 and 4.9% after 2 and 4 h, respectively. Thus, under these conditions, significant residual division takes place, but with increasing starvation time less and less of it is located at the cell poles.

The length distribution of the anucleate rods produced after 4 h of thymine starvation was measured on photomicrographs of *minB*$^+$, *minB1*, and *min-2* mutant cultures (Fig. 4 and 5). The *minB1* anucleate rods were extremely heterogeneous in size, with 30% in the form of anucleate filaments over 5 μm long, and some exceeded 13 μm in length; such cells were never observed with *minB*$^+$ strains or in the unstarved *minB1* culture. In the *min-2* strain GC7245, anucleate rods were also heterogeneous in size (data not shown). Thus, the *min* defect seems to permit aberrant division at poles and at sites far from the poles in thymine-starved filaments. The broad size distribution of anucleate rods suggests that the residual division during thymine starvation of *min* mutants occurs essentially at random along the filaments. This could account for the decrease in polar division, since the poles, whose size remains constant, represent a progressively decreasing fraction of the filament length available for septation.

The SOS response in the *minB1* mutant. The above observations suggest that the *min* defect may alter the replication, structure, or segregation of chromosomal DNA. Such defects could cause induction of the SOS response (35). We looked to see whether this was the case for the *minB1* mutant. The level of induction of the SOS response was evaluated in two ways: (i) by measuring the differential rate of β-galactosidase synthesis in strains GC7078 (*minB*$^+$) and GC7088 (*minB1*) lysogenic for the phage λ p(*sfiA*::*lac*) *cI ind* (14), which carries the *lacZ* gene fused to the promoter of the SOS operon *sfiA*, and (ii) by measuring the proportion of Gal$^+$ colonies in MT1 (*minB*$^+$) and GC7142 (*minB1*), in which the *gal* operon is fused to the rightward operon of λ, normally repressed by the λ repressor (Gal$^-$ phenotype) but maintained in a derepressed state (Gal$^+$ phenotype) after even transient inducing treatments owing to expression of the *cro* gene product, which prevents the repressor from being resynthesized (33). By both tests no significant induction of the SOS response was detected in the *minB1* mutant (data not shown). This is consistent with the observation that the *minB1* strain still produced anucleate rods in an *sfi*$^+$

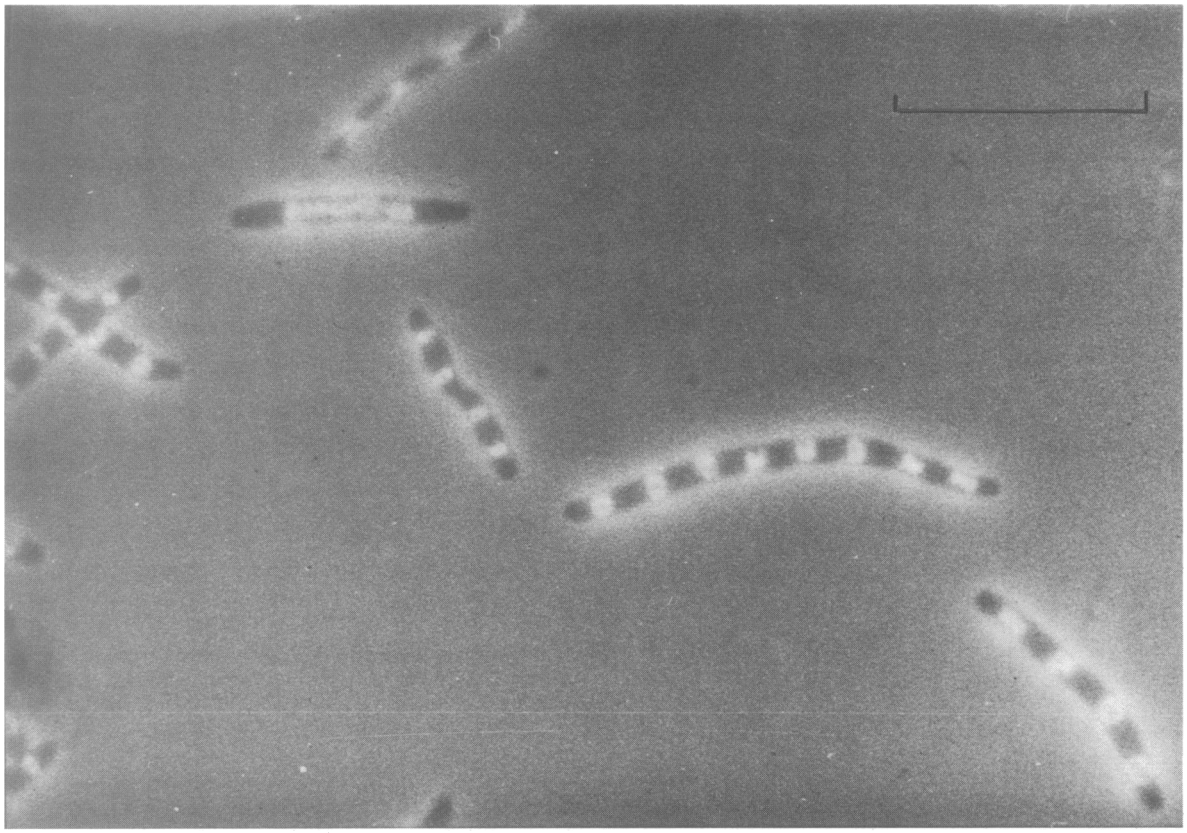

FIG. 3. DNA staining of furazlocillin-chloramphenicol-treated *min-2* cells. A culture of strain GC7245 was grown for 1 h in LB broth containing furazlocillin, followed by 1 h in chloramphenicol. DAPI staining was then carried out, and the cells were photographed. The culture contained filaments with regularly distributed nucleoids, filaments with condensed nucleoids, and minicells. Bar, 10 μm.

background, in which the SOS division inhibitor SfiA was functional (Table 2).

Effect of the cAMP-CAP complex on minicell and anucleate rod production. We have previously shown that the formation of anucleate rods during inhibition of DNA synthesis requires a functional cAMP-CAP complex (19). To test minicell and anucleate rod production by the *min* mutants in the absence of this complex, a *cya* deletion was transduced into these strains. All experiments were carried out with early-exponential-phase cultures; under these conditions, *cya* mutant cells are rod shaped (7), and minicells were readily distinguished from rods. In the *min cya* mutants, minicell formation was not inhibited, as observed by phase-contrast microscopy. In contrast, spontaneous production of anucleate rods, evaluated by autoradiography in the *minB1 cya* strain GC7082, was 10-fold lower than in the *minB1 cya*$^+$ strain (Table 2). Similarly, few anucleate rods were produced during thymine starvation (Table 2). These observations show that minicell production is not subject to the same control as anucleate rod generation: the latter requires a functional cAMP-CAP complex, both spontaneously (in the *min* mutants) and during DNA synthesis blocks (in *min*$^+$ and *min* strains), whereas minicell production is cAMP-CAP independent.

The formation of anucleate rods has been correlated with the presence of filaments with an abnormal DNA distribution. However, the *cya* mutation did not restore a normal nucleoid distribution in the *min cya* strains, as observed by fluorescence microscopy after furazlocillin and chloramphenicol treatment.

Mutants lacking cAMP (*cya*) or CAP (*crp*) grow more slowly than wild-type strains (7). This effect was enhanced in the double mutants GC7255 (*min-2 cya*) and GC7261 (*min-4 cya*), although not in GC7254 (*minB1 cya*). The *cya* deletion was introduced into the former strains by transduction in the presence of cAMP, and these double mutants grew extremely poorly in its absence.

The above results show that (i) the *min* mutants spontaneously generate anucleate rods as well as minicells of variable diameter, (ii) when DNA synthesis is blocked in the absence of SOS-associated division inhibition, similar levels of anucleate rods are produced in *min*$^+$ and *min* strains, (iii) the size distribution of the anucleate cells generated by the *min* mutants when DNA synthesis is blocked is much broader than in the *min*$^+$ strain and includes anucleate filaments, (iv) the number of visible constrictions, both polar and nonpolar, drops in the absence of DNA synthesis, (v) DNA structure or distribution appears to be altered in the *min* mutants, although the SOS response is not induced, and (vi) spontaneous generation of anucleate rods by the *min* mutants requires a functional cAMP-CAP complex, whereas (vii) minicell production is cAMP independent.

DISCUSSION

Cell division normally takes place at the cell center, after nuclear segregation has placed chromosomes in both halves of the cell. Minicell production results from an aberrant division taking place at the cell pole, with all the DNA on one side of the septum. In the present work, three new *min*

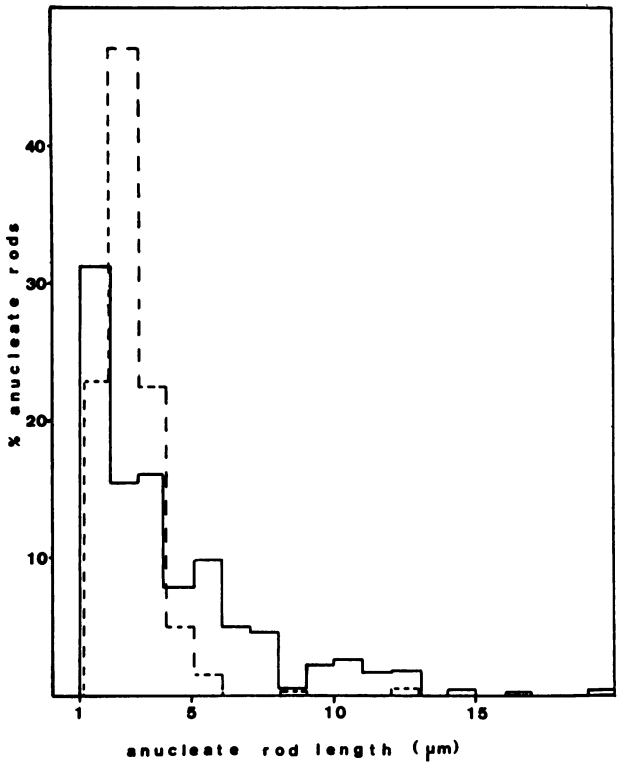

FIG. 4. Size distribution of anucleate cells in thymine-starved *minB1* and *minB*$^+$ cultures. Cultures of strains B1688 (*minB1*) and B1654 (*minB*$^+$) were starved for thymine for 4 h; autoradiography was then carried out, and the cells were photographed. The cell length of anucleate cells was measured; the ordinate represents the percentage of all anucleate rods (excluding minicells) that lay within each size class. For strain B1688 (*minB1*), 500 cells were measured (solid line), and for strain B1654 (*minB*$^+$), 200 cells were measured (dashed line).

mutants were isolated and characterized, in parallel with the *minB1* mutant isolated by Adler et al. (1), with respect to their division process, their DNA distribution, and their ability to coordinate cell division with DNA replication.

We observed that the *min* mutants spontaneously produced two types of anucleate cells, spherical minicells and anucleate rods. Both types of anucleate cells had a broad size distribution (Fig. 2). This was particularly surprising in the case of the minicells, since cell diameter is constant in our experimental conditions. The diameter of the largest minicells was equal to the length of the smallest anucleate rods (Fig. 2); if we consider the volume of each size class, the two distributions overlap extensively.

Analysis of the *min* mutants by autoradiography and DAPI staining revealed that a fraction of the filaments had an abnormal nucleoid distribution, with their DNA centrally located, and DNA-free regions extending from the poles. These cells are presumably the progenitors of anucleate rods, since constrictions were sometimes observed about 1.5 μm from the pole, with all the DNA on one side.

When cell division was inhibited by the antibiotic furazlocillin, the wild-type strain produced filaments with the nucleoids distributed uniformly from pole to pole with equal spacing, and removal of the antibiotic restored cell division but did not result in the production of anucleate rods. In furazlocillin-treated *min* mutant cultures, on the contrary, about 20% of the filaments had long DNA-free regions at both poles.

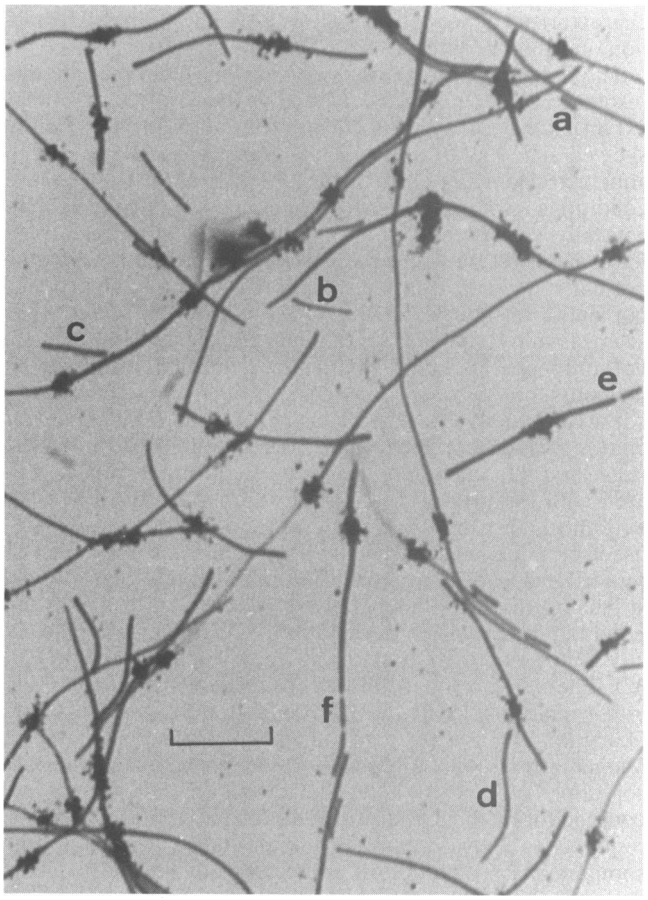

FIG. 5. Autoradiography of thymine-starved *minB1* cells. A culture of strain B1688 (*minB1*) was starved for thymine for 4 h; autoradiography was then carried out, and the cells were photographed. The culture contained normal-sized cells (a), anucleate filaments (b, c, and d), and filaments showing one (e) or two (f) constrictions. Bar, 10 μm.

Production of anucleate rods has previously been associated with DNA perturbations in the absence of SOS-associated division inhibition (19), and it seemed possible that the *min* defect might lead to this situation. We show here that the SOS response is not induced spontaneously in *minB1* strains. On the other hand, several observations suggest that *min* cultures contain a subpopulation in which DNA replication, structure, or segregation is perturbed: (i) DNA-free poles were observed occasionally in spontaneous *min* filaments but not in wild-type cultures, and (ii) some of the furazlocillin-induced *min* filaments had an irregular DNA mass distribution and condensed nucleoids, an image seen in *minB*$^+$ strains only when DNA synthesis is perturbed (28).

Anucleate rods are produced in *minB*$^+$ strains when DNA synthesis is perturbed in the absence of SOS-associated division inhibition, and this production requires a functional cAMP-CAP complex (19). The same was true in the *min* mutants: in the absence of cAMP no anucleate rods were produced, either spontaneously or during blocks in DNA synthesis. This cAMP-CAP dependence of anucleate rod production suggests that the same type of aberrant division is involved in all cases. Minicell production, on the other hand, continued in *min cya* strains and thus does not require cAMP, indicating that aberrant divisions at cell poles and within filaments are regulated differently. Another minicell-producing strain, described by Kumar et al. (23) but not

characterized genetically, requires cAMP for minicell formation and thus is different from the *min* mutants.

The inhibition of DNA synthesis in the *min* mutants resulted in the accumulation of anucleate rods to a similar extent as in *min*$^+$ strains (15 to 50%) but with a markedly skewed size distribution, ranging from cells 1.2 μm long to anucleate filaments up to 13 μm long (Fig. 4). Under these conditions *min*$^+$ cultures also contained long filaments with centrally located DNA and extended DNA-free regions at the poles, yet the only constrictions observed were one normal cell length from the pole, producing a homogeneous population of anucleate rods (Fig. 4). The *min* defect thus seems to allow aberrant septation at normally forbidden sites not only at cell poles but also at internal locations on filaments.

Previous analysis of the cell length distribution in a *minB1* culture, which contains filaments in addition to minicells, suggested that each minicell-producing division was associated with the loss of a normal division (32), leading to the hypothesis that the *minB*$^+$ function somehow "cancels out" used septation sites and that in its absence these sites can be reused (cell poles are used septation sites); this model stipulated that each unit increase in cell mass provides the potential for exactly one septation, which can take place at any of the potential sites available, chosen at random (10, 32). The *min-2* mutant differed from the *minB1*, *min-3*, and *min-4* mutants in its lower production of minicells and filaments; this suggests that minicell production parallels filamentation, compatible with the above model. Other observations presented here, however, are not readily accounted for by the model. An additional hypothesis would be required to explain how *min* mutations can lead to the spontaneous production of anucleate rods and of filaments with an abnormal nucleoid distribution. Furthermore, the heterogeneity in the size of anucleate rods and minicells, produced spontaneously or after thymine starvation, is in direct contradiction to the postulate that only normal division sites are used (or reused) in *min* strains.

The phenotype of the *min* mutants is reminiscent of that of a *gyrB*(Ts) strain (30) and of a *gyrA*(Am) strain (16, 17). In these mutants at high temperature, gyrase activity is altered, resulting in conformational changes in the DNA, with a defect in the separation into separate nucleoids; the mutants produce anucleate rods that are heterogeneous in size and minicells. These observations show that a primary defect at the level of DNA structure and DNA partitioning can indeed result in a complex phenotype which includes minicell and anucleate rod production.

ACKNOWLEDGMENTS

We thank Larry Rothfield for helpful discussions, encouragement, and strains. Laurent Guttman kindly provided us with β-lactamase, and Graham Walker and Agnes Ullmann provided us with strains. We are grateful to Willie Donachie and Conrad Woldringh for their continued interest in this work and to Antonia Kropfinger, Richard Schwartzmann, Muriel Brachet, Murielle Leconte, and Denis Brachet for preparing the text, photographs, and figures efficiently and cheerfully. We thank our colleagues Philippe Bouloc, Danièle Joseleau-Petit, Jean-Claude Liébart, Emmanuelle Maguin, Teru Ogura, and Aline Robin for their warm support.

This work was supported in part by the Association pour la Recherche sur le Cancer (grant 6696), the Fondation pour la Recherche Médicale, and the University of Kumamoto and by a Grant-in-Aid for Scientific Research on Priority Areas, a Grant-in-Aid for Scientific Research, and the Monbusho International Scientific Research Program for Joint Research from the Ministry of Education, Science and Culture, Japan.

LITERATURE CITED

1. **Adler, H. I., W. Fisher, A. Cohen, and A. Hardigree.** 1967. Miniature *E. coli* cells deficient in DNA. Proc. Natl. Acad. Sci. USA **57**:321–326.
2. **Adler, H. I., W. D. Fisher, and A. A. Hardigree.** 1969. Cell division in *Escherichia coli*. Trans. N.Y. Acad. Sci. **31**:1059–1070.
3. **Botta, G. A., and J. T. Park.** 1981. Evidence for involvement of penicillin-binding protein 3 in murein synthesis during septation but not during cell elongation. J. Bacteriol. **145**:333–340.
4. **Brickman, E., L. Soll, and J. Beckwith.** 1973. Genetic characterization of mutations which affect catabolite-sensitive operons in *Escherichia coli*, including deletions of the gene for adenyl cyclase. J. Bacteriol. **116**:582–587.
5. **Clark, D. J.** 1968. Regulation of deoxyribonucleic acid replication and cell division in *Escherichia coli* B/r. J. Bacteriol. **96**: 1214–1224.
6. **D'Ari, R., and O. Huisman.** 1983. Novel mechanism of cell division inhibition associated with the SOS response in *Escherichia coli*. J. Bacteriol. **156**:243–250.
7. **D'Ari, R., A. Jaffé, P. Bouloc, and A. Robin.** 1988. Cyclic AMP and cell division in *Escherichia coli*. J. Bacteriol. **170**:65–70.
8. **Davie, E., K. Sydnor, and L. I. Rothfield.** 1984. Genetic basis of minicell formation in *Escherichia coli* K-12. J. Bacteriol. **158**: 1202–1203.
9. **De Boer, P. A. J., R. E. Crossley, and L. I. Rothfield.** 1988. Isolation and properties of *minB*, a complex genetic locus involved in correct placement of the division site in *Escherichia coli*. J. Bacteriol. **170**:2106–2112.
10. **Donachie, W. D., K. J. Begg, and N. F. Sullivan.** 1984. Morphogenes of *Escherichia coli*, p. 27–62. *In* R. Losick and L. Shapiro (ed.), Microbial development. Cold Spring Harbor Laboratory, Cold Spring Harbor, N.Y.
11. **Fairweather, N. F., E. Orr, and I. B. Holland.** 1980. Inhibition of deoxyribonucleic acid gyrase: effects on nucleic acid synthesis and cell division in *Escherichia coli* K-12. J. Bacteriol. **142**:153–161.
12. **George, J., M. Castellazzi, and G. Buttin.** 1975. Prophage induction and cell division in *E. coli*. III. Mutations in *sfiA* and *sfiB* restore division in *tif* and *lon* strains and permit expression of mutator properties of *tif*. Mol. Gen. Genet. **140**:309–332.
13. **Huisman, O., and R. D'Ari.** 1981. An inducible DNA replication-cell division coupling mechanism in *E. coli*. Nature (London) **290**:797–799.
14. **Huisman, O., and R. D'Ari.** 1983. Effect of suppressors of SOS-mediated filamentation on *sfiA* operon expression in *Escherichia coli*. J. Bacteriol. **153**:169–175.
15. **Huisman, O., R. D'Ari, and S. Gottesman.** 1984. Cell division control in *Escherichia coli*: specific induction of the SOS function SfiA protein is sufficient to block septation. Proc. Natl. Acad. Sci. USA **81**:4490–4494.
16. **Hussain, K., K. J. Begg, G. P. C. Salmond, and W. D. Donachie.** 1987. ParD: a new gene coding for a protein required for chromosome partitioning and septum localisation. Mol. Microbiol. **1**:73–81.
17. **Hussain, K., E. J. Elliott, and G. P. C. Salmond.** 1987. The ParD$^-$ mutant of *Escherichia coli* also carries a $gyrA_{am}$ mutation: the complete sequence of *gyrA*. Mol. Microbiol. **1**:259–273.
18. **Jaffé, A., and R. D'Ari.** 1985. Regulation of chromosome segregation in *Escherichia coli*. Ann. Microbiol. (Paris) **136A**: 159–164.
19. **Jaffé, A., R. D'Ari, and V. Norris.** 1986. SOS-independent coupling between DNA replication and cell division in *Escherichia coli*. J. Bacteriol. **165**:66–71.
20. **Jaffé, A., T. Ogura, and S. Hiraga.** 1985. Effects of the *ccd* function of the F plasmid on bacterial growth. J. Bacteriol. **163**: 841–849.
21. **Jones, C., and I. B. Holland.** 1984. Inactivation of essential genes, *ftsA*, *ftsZ*, suppresses mutation at *sfiB*, a locus mediating division inhibition during the SOS response in *E. coli*. EMBO J. **3**:1181–1186.
22. **Jones, C., and I. B. Holland.** 1985. Role of the SulB (FtsZ)

protein in division inhibition during the SOS response in *E. coli*: FtsZ stabilizes the inhibitor SulA in maxicells. Proc. Natl. Acad. Sci. USA **82**:6045–6049.
23. **Kumar, S., N. Prakash, and V. K. Sharma.** 1979. Control of minicell producing cell division by cAMP-receptor protein complex in *Escherichia coli*. Mol. Gen. Genet. **176**:449–450.
24. **Lutkenhaus, J.** 1983. Coupling of DNA replication and cell division: *sulB* is an allele of *ftsZ*. J. Bacteriol. **154**:1339–1346.
25. **Maguin, E., H. Brody, C. W. Hill, and R. D'Ari.** 1986. SOS-associated division inhibition gene *sfiC* is part of excisable element e14 in *Escherichia coli*. J. Bacteriol. **168**:464–466.
26. **Maniatis, T., E. F. Fritsch, and J. Sambrook.** 1982. Molecular cloning: a laboratory manual. Cold Spring Harbor Laboratory, Cold Spring Harbor, N.Y.
27. **Miller, J. M.** 1972. Experiments in molecular genetics. Cold Spring Harbor Laboratory, Cold Spring Harbor, N.Y.
28. **Norris, V., T. Alliotte, A. Jaffé, and R. D'Ari.** 1986. DNA replication termination in *Escherichia coli parB* (a *dnaG* allele), *parA*, and *gyrB* mutants affected in DNA distribution. J. Bacteriol. **168**:494–504.
29. **Ogura, T., and S. Hiraga.** 1983. Mini-F plasmid genes that couple host cell division to plasmid proliferation. Proc. Natl. Acad. Sci. USA **80**:4784–4788.
30. **Orr, E., N. F. Fairweather, I. B. Holland, and R. H. Pritchard.** 1979. Isolation and characterization of a strain carrying a conditional lethal mutation in the *cou* gene of *Escherichia coli* K-12. Mol. Gen. Genet. **177**:103–112.
31. **Schaumberg, T. H., and P. L. Kuempel.** 1983. Genetic mapping of the *minB* locus in *Escherichia coli* K-12. J. Bacteriol. **153**: 1063–1065.
32. **Teather, R. M., J. F. Collins, and W. D. Donachie.** 1974. Quantal behavior of a diffusible factor which initiates septum formation at potential division sites in *Escherichia coli*. J. Bacteriol. **118**: 407–413.
33. **Toman, Z., C. Dambly-Chaudière, L. Tenenbaum, and M. Radman.** 1985. A system for detection of genetic and epigenetic alteration in *Escherichia coli* induced by DNA-damaging agents. J. Mol. Biol. **186**:97–105.
34. **Vogel, H. J., and D. M. Bonner.** 1956. Acetylornithinase of *Escherichia coli*: partial purification and some properties. J. Biol. Chem. **218**:97–106.
35. **Walker, G. C.** 1984. Mutagenesis and inducible response to deoxyribonucleic acid damage in *Escherichia coli*. Microbiol. Rev. **165**:66–71.
36. **Ward, J. E., Jr., and J. Lutkenhaus.** 1985. Overproduction of FtsZ induces minicell formation in *E. coli*. Cell **42**:941–949.